Sensors and Actuators B 176 (2013) 1121–1127

Contents lists available at SciVerse ScienceDirect

Sensors and Actuators B: Chemical

journal homepage: www.elsevier.com/locate/snb

Long period fiber grating based temperature-compensated high performance sensor for bio-chemical sensing applications

Ruchi Garg[a], Saurabh Mani Tripathi[b,*], Krishna Thyagarajan[a], Wojtek J. Bock[b]

[a] Department of Physics, Indian Institute of Technology Delhi, New Delhi 110016, India
[b] Centre de Recherche en Photonique, Université du Québec en Outaouais, Gatineau, Québec, Canada J8Y 3G5

ARTICLE INFO

Article history:
Received 10 July 2012
Received in revised form 22 August 2012
Accepted 26 August 2012
Available online xxx

Keywords:
Long period fiber grating
Refractometer
Temperature insensitive sensor
Spectral interrogation

ABSTRACT

We report a stable, robust, and extremely sensitive refractive index sensor based on long period gratings written in optical fibers (LPFGs). By splitting the LPFG transmission spectrum at its phase-matching turn-around point, we show that it is possible to achieve an ultra-high sensitivity (~2500 nm per refractive index unit) for biological/chemical samples. The splitting has been achieved by introducing an optical path difference of ~0.39 μm between the core and cladding modes within the grating region of the optical fiber. In contrast to the widely used surface plasmon resonance (SPR) based sensors, no bulky prism, circulator or metal deposition is required in our sensor, making the present sensor extremely accurate, very compact and cost effective. We also demonstrate that a simultaneous measurement of refractive index and temperature/strain can be carried out using this sensor.

1. Introduction

Precision refractive index (RI) sensing is of prime importance for both scientific and industrial research sectors. Being a fundamental quantity, an accurate determination of RI of an analyte is often a prerequisite for biological and chemical sensing since a number of substances can be detected through measurements of the RI. Over the years, several highly sensitive RI sensors based on long period fiber gratings (LPFGs) [1–4], surface plasmon resonance (SPR) [5], reverse symmetry waveguides (RSW) [6] and metal clad waveguides [7] *have been reported*. Although these sensors offer an extremely high sensitivity (~2000 nm/RIU; RIU: refractive index unit) the requirement of metallic film, bulky prism, and/or optical circulator, for the SPR based sensors, and special waveguide geometry for the RSW waveguides often increases the size and overall cost of the sensor. On the other hand, the LPFG based sensors, which are based on periodic refractive index modulation in the optical fiber core, are compact, easy to fabricate and do not need any metallization. The second major advantage of the LPFG based sensors is the possibility to tune the resonance wavelength anywhere in the electromagnetic spectrum including the highly sensitive infrared region. The sensitivity of the LPFG based sensors, however, is relatively smaller (~700 nm/RIU) as compared to the SPR based sensors. Typically, for biosensors the refractive index sensitivity should be of the order of 1000 nm/RIU.

LPFGs are periodic refractive index variations created within the core region of optical fiber (diameter ~9 μm) to redirect part of the optical field from the fiber core region (known as the core mode) to the cladding region (diameter ~125 μm) known as the cladding mode of the optical fiber. The specific wavelength at which the field is redirected is known as the resonance wavelength (λ_R) and is expressed as [4],

$$\lambda_R = \Lambda \left(n_{eff}^{co} - n_{eff}^{cl} + \frac{\kappa_{co-co} - \kappa_{cl-cl}}{k_0} \right) \quad (1)$$

where n_{eff}^{co} and n_{eff}^{cl} are respectively the effective refractive indices of the core and the cladding mode; Λ is the grating period; and κ_{co-co} and κ_{cl-cl} are the self-coupling coefficients of the core mode and the cladding mode, respectively. A small fraction of the cladding mode field, evanescent field, travels outside of the optical fiber, interacting with the outer region; any variations in the refractive index of the outer region will affect n_{eff}^{cl} and, thus, will change λ_R. The LPFG sensing principle primarily relies on measuring the shift in λ_R, due to the changes in the refractive index. It is well known that higher the cladding mode order, larger would be the corresponding evanescent field in the region outside the fiber, higher would be the sensitivity of the sensor.

To utilize the benefits of the LPFG based sensors in biological sensing their sensitivity must be enhanced. There have been some attempts in this direction, most notably exploiting of the optical power coupling to the higher order cladding modes leading to the phenomenon of dual resonance [8]. At dual-resonance the same cladding mode is excited at two distinct wavelengths, both of them shifting towards opposite direction with any change

* Corresponding author.
E-mail address: tripathi.sm1@gmail.com (S.M. Tripathi).

0925-4005/$ – see front matter © 2012 Elsevier B.V. All rights reserved.
http://dx.doi.org/10.1016/j.snb.2012.08.059

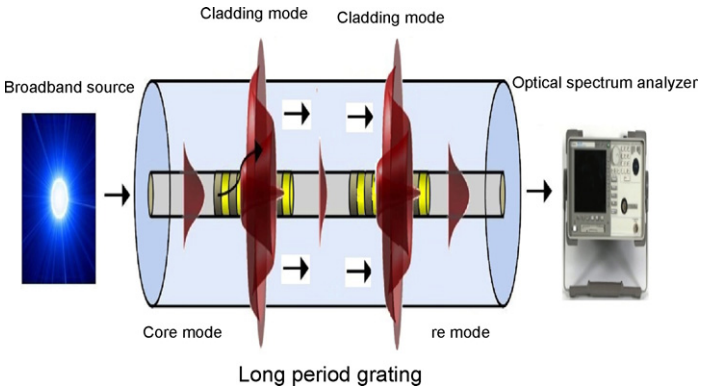

Fig. 1. Schematic of the sensor configuration.

in the analyte. This feature is of considerable interest in sensing applications because it nearly doubles the sensitivity of the LPFG based sensor [9,10]. The closer the grating period to the turn-around point (TAP) the larger is the sensitivity [11]. Recently the LPFGs, with nanostructure coatings, operating near the TAP have been experimentally demonstrated to achieve a high sensitivity [12]. Near the TAP, however, the two resonant dips coalesce to form a broad spectrum and cannot be resolved, making the spectral interrogation technique impossible. At the TAP the variations in the analyte refractive index bring out considerable changes in the LPFG transmission amplitude, making the intensity interrogation method (relatively inferior to the spectral interrogation method) the only possibility [13]. A simultaneous exploitation of sensitivity due to the relative movement of dual resonance dips and the largest spectral shift available at the turn-around point has so far not been reported.

In this paper, we report a stable, robust, and extremely sensitive refractive index sensor based on the LPFGs operating at the TAP. Rigorously optimizing the grating parameters, we show that the splitting can be achieved by introducing an optical path difference of ~0.39 μm between the core and cladding modes within the grating region of the optical fiber. This is achieved by introducing an inter-grating space (IGS) between two identical concatenated LPFGs designed at TAP (see Fig. 1). Splitting the LPFG transmission spectrum at its phase-matching TAP we obtain the highest ever reported sensitivity of the LPFGs, ~2500 nm/RIU, for refractive index changes of biological interest (1.333–1.353 RIU). Further, since a precise determination of the refractive index often needs temperature calibration also (since the refractive index of bio/chemical samples and the waveguide regions is a function of temperature), we demonstrate that unlike the SPR based sensors the present sensor is capable of a simultaneous measurement of the refractive index and the temperature.

2. Design consideration

Considering an LPFG in a single mode fiber, in order to design the sensor we first calculate the field profiles and the effective indices of the core mode and an appropriate cladding mode that exhibits a turn around behavior at the wavelength of our choice [14]. These in turn determine the required grating period (Λ) and the coupling coefficient which is given by the overlap of the transverse modal field profiles and the refractive index modulation (Δn) of the grating.

2.1. Optical fiber modes

In our simulations, we consider a single mode fiber having a core region to be made of 3.1 mol.% GeO_2 doped SiO_2 with a radius of 4.1 μm, and the cladding region made of fused SiO_2 with a radius of 62.5 μm. These parameters closely resemble the fiber parameters of the commercially available standard SMF-28^{TM} fiber. The wavelength dependent refractive indices, $n(\lambda)$ of core and cladding regions are obtained by using the well known Sellmeier relation given by:

$$n(\lambda^2) = 1 + \sum_{i=1}^{3} \frac{A_i \lambda^2}{(\lambda^2 - \lambda_i^2)^2}. \quad (2)$$

The Sellmeier coefficients corresponding to the core and cladding compositions are $A_1 = 0.6961663$, $A_2 = 0.4079426$, $A_3 = 0.8974794$, $\lambda_1 = 0.0684043$, $\lambda_2 = 0.1162414$, $\lambda_3 = 9.896161$ and $A_1 = 0.7028554$, $A_2 = 0.4146307$, $A_3 = 0.8974540$, $\lambda_1 = 0.0727723$, $\lambda_2 = 0.1143085$, $\lambda_3 = 9.896161$, respectively, [15] with both the λ and λ_i in the units of μm. The total field within the coupled region can be written as [14]:

$$E(x, y, z) = a_{co}(z)\,\Psi_{co}(x, y)\,e^{i\beta_{co}z} + a_{cl}(z)\,\Psi_{cl}(x, y)\,e^{i\beta_{cl}z} \quad (3)$$

where Ψ_{co}, Ψ_{cl} are the power normalized transverse field distributions, $\beta_{co}(= n_{eff}^{co} k_0)$ and $\beta_{cl}(= n_{eff}^{cl} k_0)$ are the propagation constants of the core mode and the cladding mode, respectively, and the a_{co}, a_{cl} are the modal amplitudes of the modes as denoted by the subscripts for core and the cladding mode, respectively. The effective refractive indices (n_{eff}^{co} and n_{eff}^{cl}) and the field distributions (Ψ_{co} and Ψ_{cl}) are obtained by solving the scalar Helmholtz equation [14] satisfying the continuity of the fields and its first radial derivative at all the dielectric boundaries. Fig. 2(a) and (b) shows the transverse field distributions for the participating fundamental core mode (LP_{01}) and the 9th cladding mode (LP_{010}) at the telecommunication wavelength 1.55 μm and at an ambient refractive index 1.33, respectively. The corresponding effective indices of the core and cladding modes are 1.445869 and 1.439256, respectively. The inset of Fig. 2(b) clearly shows that a finite fraction of the cladding mode field is present beyond the cladding/analyte boundary (beyond $r = 62.5$ μm).

2.2. Grating parameters and transmitted power

In order to study the power transmission characteristic of the LPFG we use the standard coupled mode theory [14]. The relationship between the amplitudes of the fields of the core and the cladding modes at any value $z = L_g$ can be written in terms of their values at $z = 0$ in the following matrix form:

$$\begin{bmatrix} a_{co}(z = L_g) \\ a_{cl}(z = L_g) \end{bmatrix} = T_{LPFG} \times \begin{bmatrix} a_{co}(z = 0) \\ a_d(z = 0) \end{bmatrix} \quad (4)$$

Here, T_{LPFG} represents the transfer matrix of the LPFG with grating length L_g, and can be written as [4],

$$T_{LPFG} = \begin{bmatrix} \cos(\gamma L_g) - i\frac{\delta}{\gamma}\sin(\gamma L_g) & -i\frac{\kappa}{\gamma}\sin(\gamma L_g) \\ -i\frac{\kappa}{\gamma}\sin(\gamma L_g) & \cos(\gamma L_g) + i\frac{\delta}{\gamma}\sin(\gamma L_g) \end{bmatrix} \quad (5)$$

where κ is the cross coupling coefficient between the core and the cladding mode given by:

$$\kappa = \frac{\omega \epsilon_0 n_{co}}{2} \int_0^{\infty} \int_0^{2\pi} \Delta n \Psi_{co} \Psi_{cl}^* r\, dr d\theta. \quad (6)$$

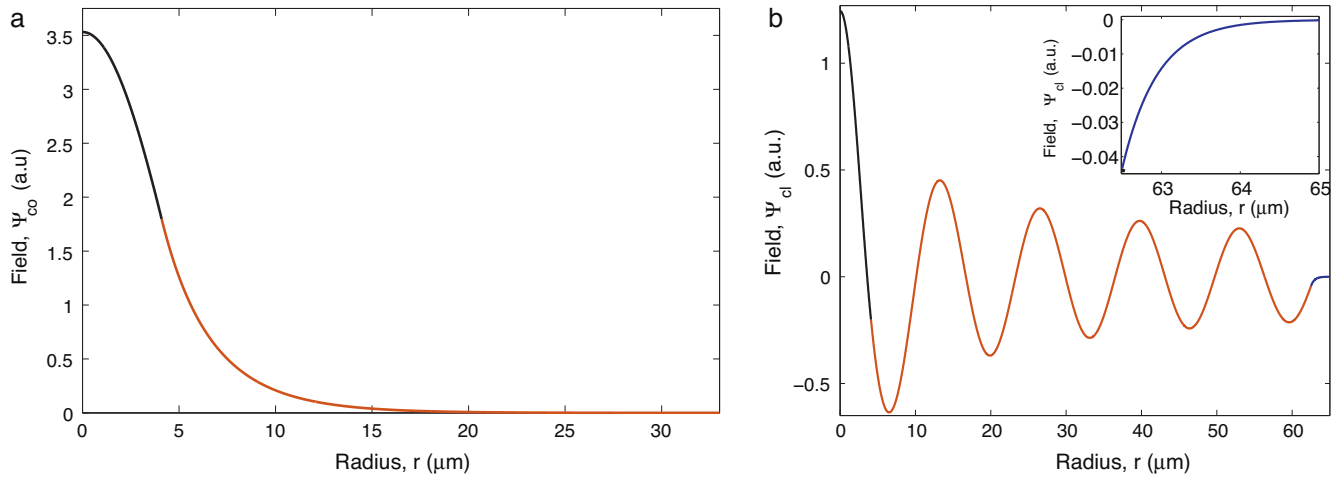

Fig. 2. Transverse field plots of the participating modes: (a) LP_{01} core mode and (b) LP_{010} cladding mode with inset showing the existence of finite cladding mode field beyond the cladding radius.

with ϵ_0(= 8.85 × 10^{-12} F/m) being the permittivity of free space and Δn the grating induced refractive index variation in the core having a refractive index n_{co}. In (5) δ is the detuning parameter given by,

$$\delta = \frac{1}{2}\left(\beta_{co} - \beta_{cl} + \kappa_{co-co} - \kappa_{cl-cl} - \frac{2\pi}{\Lambda}\right) \tag{7}$$

with $\gamma = \sqrt{\kappa^2 + \delta^2}$.

For an initial condition that the entire power is being launched only in the core mode, we have $a_{co}(z=0) = 1$ and $a_{cl}(z=0) = 0$; substituting in Eq. (4) and using Eq. (5) we can obtain the transmitted amplitude of the core mode $a_{co}(z = L_g)$ from which we can obtain the transmitted power *P*.

Corresponding to the fiber parameters specified above, the phase matching curve between the LP_{01} core mode and the LP_{010} cladding mode, obtained for a zero detuning ($\delta = 0$), is plotted in Fig. 3(a) for two analyte refractive indices. The phase matching curve shows maximum shift at the turn-around point wavelength, λ_{TAP} ~1.56 μm when ambient index changes from, n_{se} = 1.33 to n_{se} = 1.335. Fig. 3(a) clearly reveals that the largest sensitivity is possible only at the turn-around point grating period. The transmission spectrum obtained for two different grating periods (i) at the turn-around point (Λ = 230.89 μm) and (ii) away from the turn-around point (Λ = 230.5 μm), are plotted in Fig. 3(b) for both the analyte refractive indices. It is evident from the figure that at the turn-around point, the two resonance (reference) wavelengths (λ_i) merge forming a single broader resonance dip, posing a limit for the TAP gratings use as a sensor. The TAP gratings have, therefore, a very limited role in sensing and are widely used as broadband stop filters [16].

2.3. Transmission spectrum splitting at the TAP

To utilize the full potential of the TAP gratings, splitting the transmission spectrum at the turn-around point is essential. This can be done by introducing an extra optical-path difference between the core mode and the cladding mode by means of an inter-grating-space (IGS). The resulting dual-resonance LPFG-IGS dual-resonance LPFG structure (Fig. 1) will behave as a Mach–Zehnder interferometer with the IGS responsible for introducing a wavelength dependent phase difference between the interfering core and cladding modes. Over years, several other Mach–Zehnder interferometer sensors based on the grating coupled interferometry [17,18] and the two-branch integrated optical waveguide MZI [19] have been reported to realize highly sensitive refractive index/affinity sensors. However, the sensor proposed here has a number of advantages over the other MZI based sensors, these advantages include (i) Ease of fabrication: both the grating coupled interferometry as well as two-branch integrated optical waveguide MZI require complex waveguide fabrication facilities; whereas the LPFG can be easily fabricated in the widely available standard telecommunication grade single mode fibers. (ii) Ease of operation: unlike the grating coupled interferometry and the two-branch integrated optical waveguide MZI, no grating coupler or pig-tailing is required to couple the optical wave to the waveguide. (iii) Extremely high sensitivity: the LPFG-IGS dual resonance sensor proposed here utilizes the merits of an extremely high sensitivity achievable at the turn-around point. The resulted sensitivity (2500 nm/RIU) when used with the peak/dip finding algorithm and a detection system with a spectral resolution of 1 pm, is capable of measuring changes as small as 4 × 10^{-7} RIU in the analyte as compared to the 10^{-5} RIU offered by the standard Grating coupled interferometry sensors. As we discuss in the following, by adjusting this optical-path difference the transmission spectrum can be split and the losses associated with the two resonance wavelengths can be adjusted to the desired value.

The transmitted amplitude through the above structure can be obtained by introducing a phase matrix T_{IGS} to incorporate the phase difference developed within the IGS region. The overall transmission of the structure can be described by the following equation:

$$T = T_{LPFG2} \times T_{IGS} \times T_{LPFG1} \times \begin{bmatrix} 1 \\ 0 \end{bmatrix} \tag{8}$$

where for an IGS = L_{IGS} the phase matrix T_{IGS} is given as

$$T_{IGS} = \begin{bmatrix} e^{i\beta_c L_{IGS}} & 0 \\ 0 & e^{i\beta_{cl} L_{IGS}} \end{bmatrix} \tag{9}$$

Using Eq. (8), the influence of the phase difference ($\phi = (\beta_c - \beta_{cl})L_{IGS}$) on the transmitted power of the core mode has been simulated and shown in Fig. 4. Phase difference $\phi = 0$ is represented by the solid curve in the figure and corresponds to no inter-grating space. A broad attenuation band in the transmission spectrum is observed due to the two unresolved transmission minima. In the presence of a phase difference, due to the inter-grating spacing, the central-broad band starts splitting into two dips. This splitting gets further enhanced as the phase difference is increased. The dashed curve shows well-separated two attenuation dips for gratings designed at the turning point with an inter-grating space

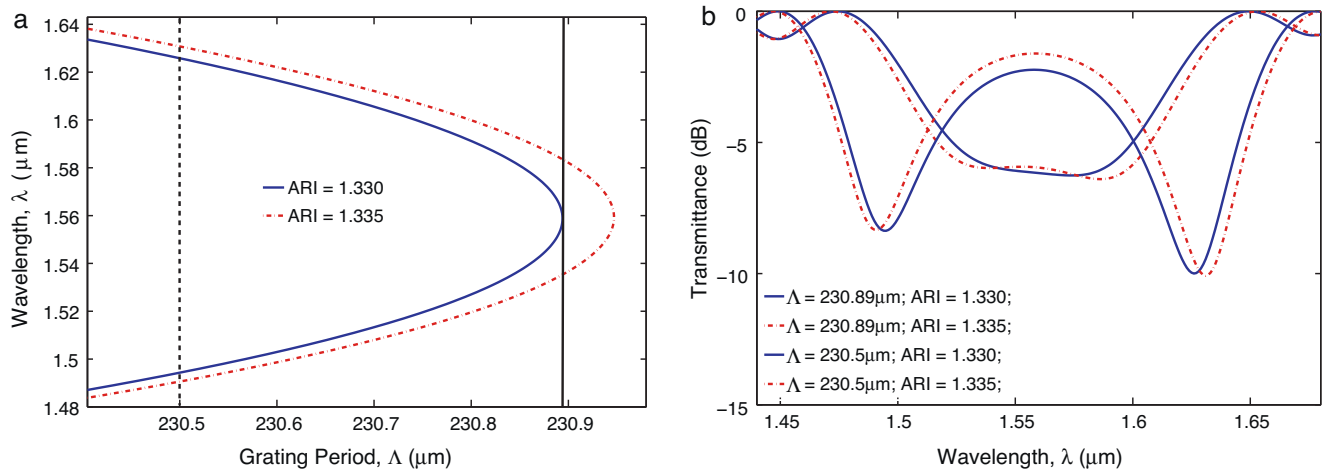

Fig. 3. A comparison between the gratings designed at two different periods for two analyte refractive indices. (a) Phase matching curves. (b) Transmission spectra.

causing a phase difference of $\phi = \pi/2$. The dot-dashed curve shows the transmission spectrum at $\phi = \pi$. The evolution of these attenuation dips is a periodic phenomenon which means that increasing the phase difference beyond π results in the reemergence of the central dip and the whole process repeats periodically with 2π. The dotted curve in Fig. 4 shows the reemerging broad attenuation band in the transmission spectrum. For practical purposes, a smaller inter-grating space is desirable to minimize the wastage of the biological samples. Referring to Fig. 4, we choose the parameter of our requirement as $\phi = \pi/2$, with the corresponding IGS being ~70 μm (the optical-path difference being ~0.39 μm).

Having calculated the necessary optical-path difference between the core mode and the cladding mode to split the transmission spectrum, in the following we discuss the fabrication and characterization of the turn-around LPFG biosensor.

3. Experimental results and discussion

3.1. TAP-LPFG fabrication

To carry out the experiments we fabricated several highly sensitive LPFGs in the single mode optical fiber SMF-28™ (Corning: NY, 14831 USA). For ease of fabrication the photosensitivity of the fibers was first increased by hydrogen loading of the fibers at 150 bars in hydrogen chamber for 15 days. Photosensitive LPFGs were then inscribed into the fiber core using KrF excimer laser operating at wavelength 248 nm with pulse repetition rate of 100 Hz, pulse duration of 12 ns and peak pulse energy of 10 mJ. In order to release excess of hydrogen, long period gratings were then annealed at 150 °C for duration of 4 h. This stabilizes the optical properties of LPFGs. The fabricated LPFGs exhibited resonance wavelength at ~1.56 μm in the presence of air as surrounding medium. In the desired aqueous solutions, the resonance wavelength shifts by ±350 nm. To achieve resonance wavelength close to the turn-around point ~1.58 μm, cladding of the fiber has been etched out gradually in 4% HF for ~3 h. This shifted the λ_R close to its turning point ~1.58 μm, enhancing the sensitivity of the LPFGs [11]. Having established the protocol to obtain the TAP LPFG, we fabricated two TAP LPFGs with varying IGS between 70 μm to 120 μm. After the HF etching we observed that, in contrast to the theoretical predictions, the well resolved resonance dips (corresponding to an optical-path difference of ~0.39 μm) are observed for an IGS of ~100 μm as shown in Fig. 5. This can be attributed to a small uncertainty in the fiber and grating parameters that have been used in the simulations.

The presence of macrobends along the grating region is the primary cause of measurement errors in LPFG based sensors. In order

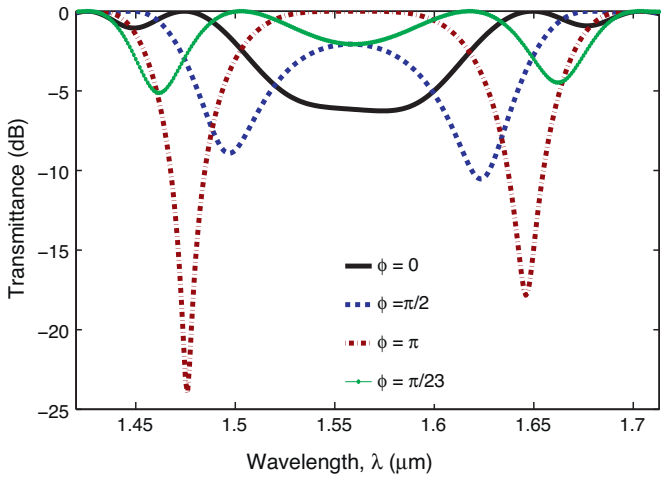

Fig. 4. Transmission spectra of the LPFG with IGS for different phase difference introduced between the core and the cladding modes.

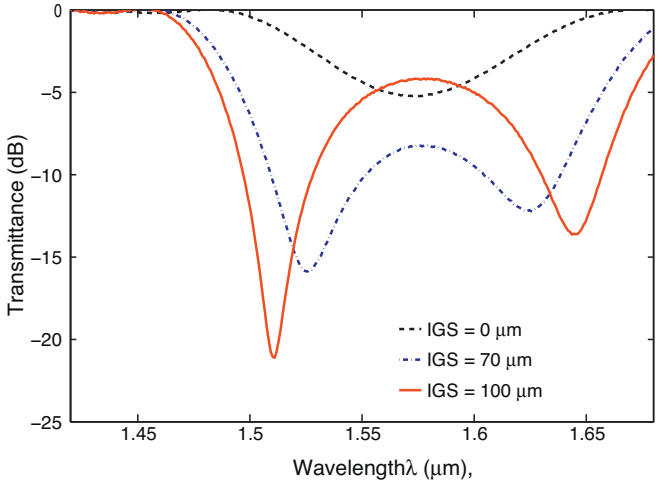

Fig. 5. Measured transmission spectra with concatenated dual resonance LPFGs for different inter-grating spacing.

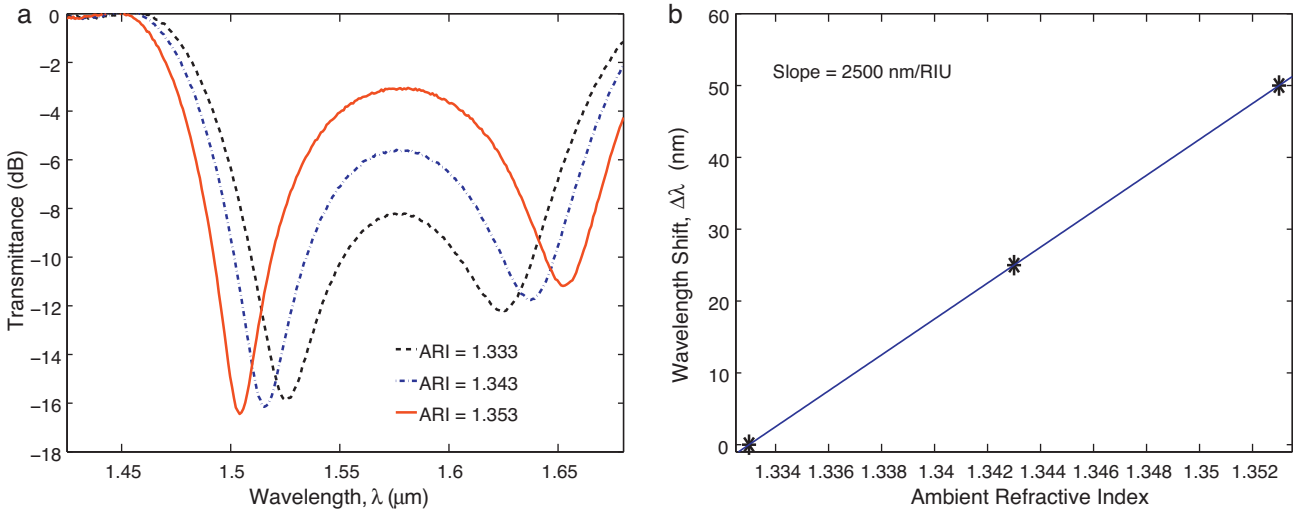

Fig. 6. Ambient refractive index sensor: (a) Transmission spectra corresponding to three different ambient refractive indices. (b) Variation of wavelength shift with respect to the analyte refractive index.

to avoid them we maintained a constant tension along the grating throughout the experiments by attaching the fiber near one end of the LPFG and applying a fixed force near the other end of it. Light was launched into the fiber using an Agilent-83437A broadband source (BBS) and the transmission spectrum was recorded using an Agilent-86142B optical spectrum analyzer (OSA) with a resolution of 0.02 nm.

3.2. Refractive index sensing

Samples of different refractive indices were prepared dissolving various concentrations of sucrose in distilled water. The refractive indices of the analytes were then measured by an Abbe refractometer (Atago DR-M2) operating at $\lambda = 1.55\,\mu m$. To observe the refractive index sensitivity due to the surrounding medium, the ideal conditions of no changes in temperature and strain have been ensured with the variation in the refractive index.

Throughout our measurements the ambient temperature has been maintained at 22 (±0.1) °C. After each measurement, prior to the next observation, the LPFGs were thoroughly washed in distilled water to remove any surface film at the fiber surface. The measured transmission spectra with respect to three different analyte refractive indices namely 1.333, 1.343 and 1.353, are shown by dashed, dot-dashed and solid lines, respectively, in Fig. 6(a). Fig. 6(b) shows a linear variation of wavelength shift with respect to changes in the analyte refractive index yielding an experimental refractive index sensitivity of ~ 2500 nm/ARI. Such sensitivity is, in our opinion, the highest reported sensitivity so far for an LPFG operating in the refractive index range of biological importance (1.333–1.353 RIU). We would like to mention here that for our sensor, with its current IGS, the maximum refractive-index shift could be measured approximately up to 1.365. This limit is imposed upon due to a fixed inter-grating space, for which the phase difference introduced between the core mode and the cladding mode starts decreasing with increasing analyte refractive indices. For high analyte refractive indices, it leads to the re-emergence of the central broad band. The maximum refractive index limit, however, can be easily increased close the cladding refractive index (~1.444) by increasing the inter-grating space. For even higher analyte refractive indices, it can be further increased by using thin high-index over-layers [20] and adjusting the inter-grating space accordingly.

3.3. Strain sensing

For the strain sensitivity measurements, we fixed one end of the fiber (near the LPFG) to a stationary stage, the other end (near the LPFG) was fixed on a micro-positioner. The LPFG was then incubated in an analyte of refractive index 1.333 (to ensure the dual-resonance) and the LPFG was subjected to computer controlled microstrain ($\mu\epsilon$) in the steps of 5 $\mu\epsilon$. The temperature was once again kept constant at 22 (± 0.1) °C throughout the measurements. Fig. 7(a) shows the transmission spectra for different strain values at constant ambient refractive index and temperature. The linear variation of experimental data, for three different axial strains namely 0 $\mu\epsilon$, 500 $\mu\epsilon$ and 950 $\mu\epsilon$, is shown in Fig. 7(b). The experimentally measured strain sensitivity comes out to be 37 pm/$\mu\epsilon$.

3.4. Temperature sensing

For the temperature sensitivity measurements, we once again immersed the LPFG to an analyte of refractive index 1.333 and heated the LPFG-containing flow-cell using a computer controlled heater in the steps of 10 (± 0.1) °C. Prior to each measurement, we waited for about 25 min to insure a constant temperature throughout the LPFG cross section. In Fig. 8(a) we show the transmission spectra for four different temperatures namely 22 °C, 32 °C, 42 °C and 52 °C, respectively. Fig. 8(b) shows the linear dependence of experimental sensitivity giving an experimental sensitivity as 1.63 nm/°C.

3.5. Simultaneous refractive index – temperature and refractive index – strain sensing

The resonance wavelength shift is influenced not only by the changing refractive index of the solution but also by other physical parameters affecting the analyte refractive index (for example the temperature) or the fiber parameters (for example axial strain). The shifts in resonance wavelength ($\Delta\lambda_R$), arising due to a change in the ARI (Δn_{ARI}) and the other perturbation parameter ($\Delta\chi$) can be expressed as:

$$\Delta\lambda_R = \left[-\Lambda\frac{\partial n_{eff}^{0m}}{\partial n_{ARI}}\right]\Delta n_{ARI} + \left[n_{eff}^{01} - n_{eff}^{0m}\frac{\partial\Lambda}{\partial\chi} + \Lambda\frac{\partial\left(n_{eff}^{01} - n_{eff}^{0m}\right)}{\partial\chi}\right]\Delta\chi \quad (10)$$

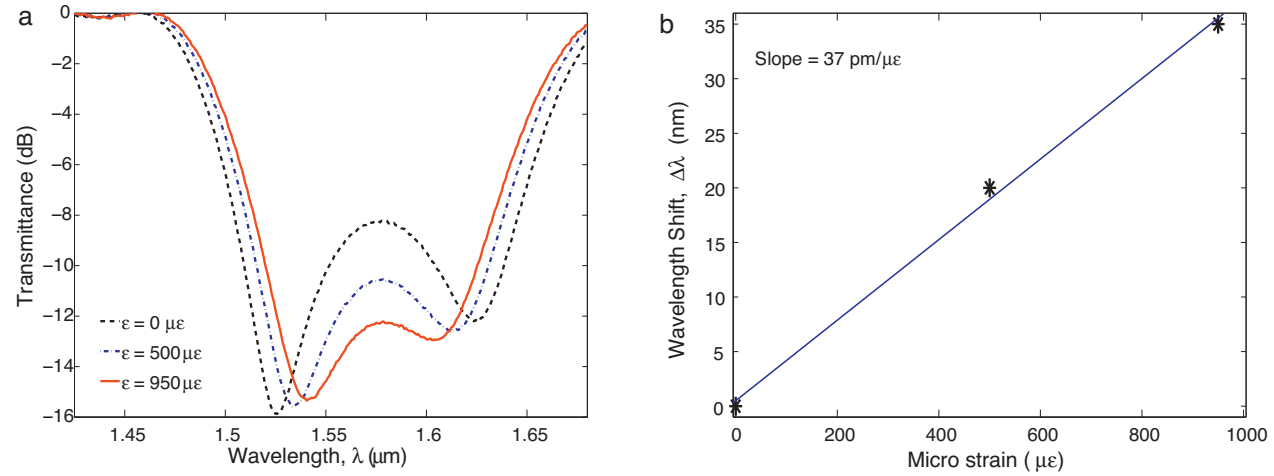

Fig. 7. Strain sensor: (a) Measured transmission spectra. (b) Variation of wavelength shift with different strain values.

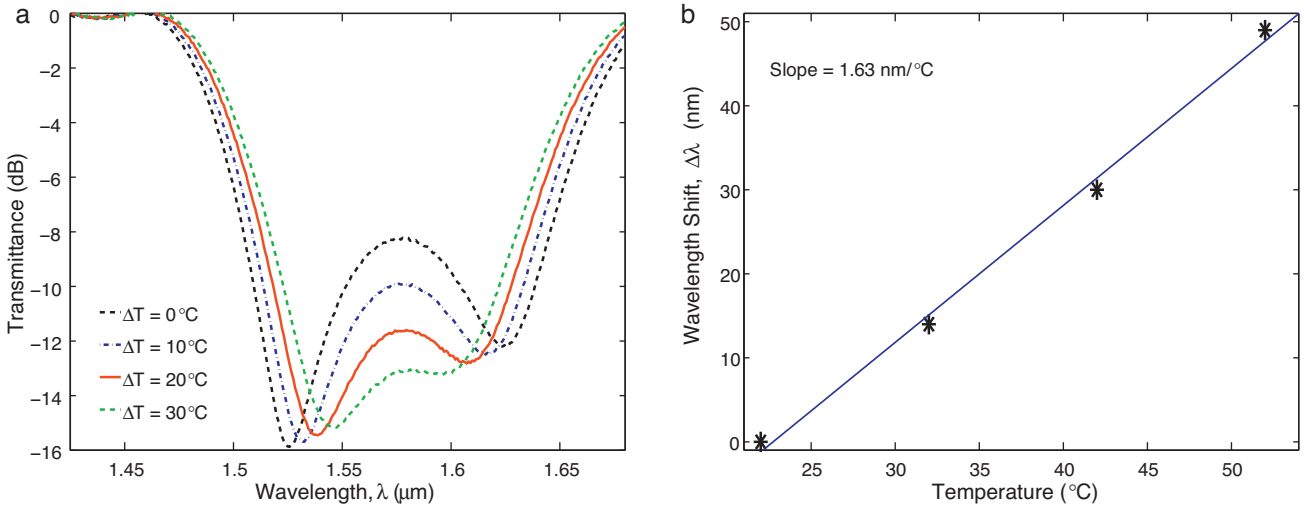

Fig. 8. Temperature sensor: (a) Measured transmission spectra. (b) Variation of wavelength shift with different temperature values.

where we have disregarded the self-coupling terms as a first-order perturbation [4]. Thus, the spectral shift of the individual resonance dips can be written as

$$\begin{bmatrix} \Delta\lambda_1 \\ \Delta\lambda_2 \end{bmatrix} = \begin{bmatrix} \frac{\partial\lambda_1}{\partial n_{ARI}} & \frac{\partial\lambda_1}{\partial\chi} \\ \frac{\partial\lambda_2}{\partial n_{ARI}} & \frac{\partial\lambda_2}{\partial\chi} \end{bmatrix} \times \begin{bmatrix} \Delta n_{ARI} \\ \Delta\chi \end{bmatrix} \tag{11}$$

For a non trivial solution, the determinant of the sensitivity matrix must not vanish, which is guaranteed by the fact that the sensitivities with respect to the temperature (strain) and refractive index, respectively, are not proportional to each other, for the two resonance wavelengths. Using the individual sensitivities of the resonance wavelengths, obtained from Figs. 6(a) and 8(a), we calculate the sensitivity matrix as,

$$M = \begin{bmatrix} -1083.3 & 0.71067 \\ 1343.3 & -0.95333 \end{bmatrix} \tag{12}$$

. Similarly, a non-vanishing determinant can also be obtained for the simultaneous measurement of refractive index and strain. Thus, by using the sensitivities of the individual dips, from Figs. 6–8, in Eq. (11) a simultaneous measurement of the changes in the external refractive index and temperature (strain) can be carried out. Here, it is important to mention that in order to ensure that the 2 × 2 cross matrix appearing in Eq. (11) is well-conditioned for an accurate measurement of the ARI, the temperature (strain) change range should not be large. To establish a relation between the allowed temperature (strain) range for an accurate simultaneous measurements, let us assume a detector system with a wavelength resolution of 1 pm. Using such a detector the minimum detectable change (=1/Sensitivity) for the ARI, temperature and the strain comes out to be $\sim 4 \times 10^{-7}$ RIU, 0.0006 °C and 0.03 με, respectively. This implies that the temperature (strain) should be limited within ±3 °C (±150 με) if the measurement range of the external RI is about 0.004 RIU. Measuring the difference and mean value of the wavelength shifts of the two resonance dips is further advised to increase the accuracy of the measurements.

4. Conclusions

In this paper we have presented a stable, robust, and extremely sensitive refractive index sensor based on the long period gratings in optical fibers. We ingeniously split the LPFG transmission spectrum at its phase-matching turn-around point, by

introducing an optical path difference of ~0.39 μm between the core and cladding modes, and have demonstrated an ultra-high sensitivity ~2500 nm per refractive index unit for the biological/chemical samples. The reported sensitivity is the highest ever reported for the LPFG based sensors and is comparable to that of the SPR based sensors. Though, in contrast to the SPR based sensors, no bulky prism or metallization is required in our sensor making them an ideal choice for biological sensing measurements. We also demonstrate that, owing to the two reference points, a simultaneous measurement of refractive index and temperature/strain can be carried out using the present sensor.

Acknowledgments

R.G. would like to thank the CSIR, India, CSIR, India, and W.J.B. acknowledge support for this work from the Natural Sciences and Engineering Research Council of Canada and Canada Research Chairs Program.

References

[1] V. Bhatia, Applications of long-period gratings to single and multi-parameter sensing, Optics Express 4 (11) (1999) 457–466.
[2] H.J. Patrick, A.D. Kersey, F. Bucholtz, Analysis of the response of long period fiber gratings to external index of refraction, Journal of Lightwave Technology 16 (September (9)) (1998) 1606–1612.
[3] V. Bhatia, A.M. Vengsarkar, Optical fiber long-period grating sensors, Optics Letters 21 (9) (1996) 692–694.
[4] R. Kashyap, Fiber Bragg Gratings, Optics and Photonics Series. Elsevier Science, 2009.
[5] J. Homola, Surface Plasmon Resonance Based Sensors, Springer Series on Chemical Sensors And Biosensors. Springer, 2006.
[6] R. Horvath, L.R. Lindvold, N.B. Larsen, Reverse-symmetry waveguides: theory and fabrication, Applied Physics B: Lasers and Optics 74 (2002) 383–393, http://dx.doi.org/10.1007/s003400200823.
[7] N. Skivesen, R. Horvath, S. Thinggaard, N.B. Larsen, H.C. Pedersen, Deep-probe metal-clad waveguide biosensors, Biosensors and Bioelectronics 22 (7) (2007) 1282–1288.
[8] S.M. Tripathi, E. Marin, A. Kumar, J.-P. Meunier, Refractive index sensing characteristics of dual resonance long period gratings in bare and metal-coated d-shaped fibers, Applied Optics 48 (31) (2009 Nov) G53–G58.
[9] X. Shu, X. Zhu, Q. Wang, S. Jiang, W. Shi, Z. Huang, D. Huang, Dual resonant peaks of lp015 cladding mode in long-period gratings, Electronics Letters 35 (8) (1999 apr) 649–651.
[10] X. Shu, X. Zhu, S. Jiang, W. Shi, D. Huang, High sensitivity of dual resonant peaks of long-period fibre grating to surrounding refractive index changes, Electronics Letters 35 (September (18)) (1999) 1580–1581.
[11] X. Shu, L. Zhang, I. Bennion, Sensitivity characteristics of long-period fiber gratings, Journal of Lightwave Technology 20 (February (2)) (2002) 255–266.
[12] C.S. Cheung, S.M. Topliss, S.W. James, R.P. Tatam, Response of fiber-optic long-period gratings operating near the phase-matching turning point to the deposition of nanostructured coatings, Journal of the Optical Society of America B 25 (6) (2008) 897–902.
[13] Z. Wang, S. Ramachandran, Ultrasensitive long-period fiber gratings for broadband modulators and sensors, Optics Letters 28 (24) (2003) 2458–2460.
[14] A.K. Ghatak, K. Thyagarajan, An Introduction to Fiber Optics, Cambridge University Press, 1998.
[15] J. Adams, An Introduction to Optical Waveguides, Wiley-Interscience Publication. Wiley, 1981.
[16] S. Ramachandran, S. Ghalmi, Z. Wang, M. Yan, Band-selection filters with concatenated long-period gratings in few-mode fibers, Optics Letters 27 (19) (2002) 1678–1680.
[17] P. Kozma, A. Hamori, K. Cottier, S. Kurunczi, R. Horvath, Grating coupled interferometry for optical sensing, Applied Physics B: Lasers and Optics 97 (2009) 5–8, http://dx.doi.org/10.1007/s00340-009-3719-1.
[18] P. Kozma, A. Hmori, S. Kurunczi, K. Cottier, R. Horvath, Grating coupled optical waveguide interferometer for label-free biosensing, Sensors and Actuators B: Chemical 155 (2) (2011) 446–450.
[19] R.G. Heideman, P.V. Lambeck, Remote opto-chemical sensing with extreme sensitivity: design, fabrication and performance of a pigtailed integrated optical phase-modulated machzehnder interferometer system, Sensors and Actuators B: Chemical 61 (13) (1999) 100–127.
[20] P. Pilla, A. Sandomenico, V. Malachovsk, A. Borriello, M. Giordano, A. Cutolo, M. Ruvo, A. Cusano, A protein-based biointerfacing route toward label-free immunoassays with long period gratings in transition mode, Biosensors and Bioelectronics 31 (1) (2012) 486–491.

Biographies

Ruchi Garg was born in Haryana, India, on November 19, 1984. She received the B.Sc. and M.Sc. degrees in Physics from University of Delhi, Delhi, India, in 2006 and 2008, respectively. Since 2008, she is a Ph.D. student at Indian Institute of Technology Delhi, India. Her research interests are in the areas of design and analysis of optical waveguide devices, long period gratings and sensors.

Dr. Saurabh Mani Tripathi obtained his Ph.D. degree in Fiber and Integrated Optics from the Indian Institute of Technology Delhi (IIT Delhi), India, in 2010, where he was a Senior Research Fellow since 2007. He carried out part of his research work at the Laboratory Hubert Curien, St-Etienne, France, during 2007–2009 where he was an Eiffel Excellence Fellow during 2008–2009. He has co-authored more than 35 scientific papers in various international journals and conferences. His research interests include biological and chemical sensors, optical waveguide gratings and modal interference based guided wave devices, integrated optical devices, and surface Plasmon polariton based sensors.

Dr. Krishna Thyagarajan joined the Physics Department at IIT Delhi in 1977 and has been a Professor of Physics, IIT Delhi since 1990. He has held Visiting positions at *Thomson-CSF*, France, *University of Florida*, USA, *University of Nice*, France, *University of Waterloo*, Canada, *City University of Hong Kong* and *Tokyo Institute of Technology*. He has published more than 140 research papers in international journals, has filed five patent applications and is the co-author (with Professor A.K. Ghatak) of seven books the latest being *Lasers: Fundamentals and Applications*, K. Thyagarajan and Ajoy Ghatak. In 1998 he was the co-recipient of the *"Fiber Optic Person of the Year 1997"* award by Lucent Technologies-Finolex and Voice and Data, India. In 2003 he was decorated with the title of *"Officier dans l'ordre des Palmes Académiques"* by the French Government. In 2005 he was elected a *Fellow of the Optical Society of America* and in 2008 he was elected a *Fellow of the Indian National Academy of Engineers*. He was a consultant to *Tejas Networks India Pvt. Ltd.*, Bangalore looking into advanced issues related to high capacity communication through optical fibers and is on the Board of Advisors to the company *"Fiber Optika"*, Bangalore. He received the *"Teaching Excellence"* award from IIT Delhi in 2009. His current research interests are in the fields of guided wave quantum optics, optical fiber amplifiers and nonlinear optical effects in photonic bandgap structure.

Dr. Wojtek J. Bock Bock received the M.Sc. degree in Electrical Engineering and the Ph.D. degree in Solid State Physics from the Warsaw University of Technology, Poland, in 1971 and 1980, respectively. Since 1989 he is a Full Professor of Electrical Engineering at the Université du Québec en Outaouais (UQO), Canada. Since 2003 Dr. Bock is Canada Research Chair Tier-I in Photonic Sensing Technologies and Director of the Photonics Research Center at UQO.

His research interests include fiber optic sensors and devices, multisensor systems, and precise measurement systems of non electric quantities. His current research program centers around developing a variety of novel fiber-optic device solutions and sensing techniques with a view to acquiring better performing photonic sensing components, devices and systems for applications in sectors of national importance to Canada. He has authored and co-authored more than 350 scientific papers, patents and conference papers in the fields of fiber optics and metrology which have been widely cited.

Dr. Bock is a Fellow of IEEE, and Associated Editor of IEEE/OSA Journal of Lightwave Technology and International Journal of Optics. "He was Chairman of the International Optical Fiber Sensor Conference (OFS21) held in Ottawa in May 2011."